JOURNAL OF GEOPHYSICAL RESEARCH, VOL. 106, NO. D17, PAGES 20,225–20,238, SEPTEMBER 16, 2001

# Modeling coastal aerosol transport and effects of surf-produced aerosols on processes in the marine atmospheric boundary layer

Elisabetta Vignati[1]

Risø National Laboratory, Roskilde, Denmark
National Environmental Research Institute, Roskilde, Denmark

Gerrit de Leeuw

Physics and Electronics Laboratory, TNO, The Hague, Netherlands

Ruwim Berkowicz

National Environmental Research Institute, Roskilde, Denmark

**Abstract.** The Coastal Aerosol Transport (CAT) model was developed to study the evolution of aerosol particle size distributions and composition in the coastal environment. The model simulates such processes as particle production at the sea surface, mixing of particles through the boundary layer by turbulent diffusion, gravitational settling, and dry deposition. The model is initialized at the shoreline with continental and/or surf aerosol. An empirical source function was developed which better accounts for the production of submicron particles than current formulations. Continental and sea spray particles are treated separately to account for effects of processes depending on chemical composition. CAT has been tested by comparison with independent data sets as regards the prediction of particle size distributions, the wind speed dependence of sea-salt aerosol mass concentrations, and the evolution of sea spray aerosol plumes generated over the surf zone. The model was applied to study effects of sea spray aerosol produced in the surf zone on sea spray concentrations, the composition of continental/sea spray aerosol mixture, the uptake of nitric acid by sea spray aerosol, and the effect of the latter process on nitric acid profiles. The results lead to the conclusion that surf-produced aerosol cannot be neglected in studies of processes involving sea spray aerosol in the coastal atmospheric boundary layer.

## 1. Introduction

The coastal environment is a special case as regards aerosol properties. At the land-sea transition, aerosol sources and sinks change abruptly, in addition to the sudden change in the surface properties, and thus in turbulent mixing and aerosol transport. Sea spray aerosol is produced only at the sea surface, while the primary production of rural, and most of the anthropogenic, aerosol, takes place over land. On either side of the coastline, these two types of aerosols are mixed and supplemented by secondary production. However, the surf zone can also be an intensive source of sea spray aerosol [*De Leeuw et al.*, 2000a] or formation of new particles at low tide [e.g., *O'Dowd et al.*, 1999]. In addition, also sources for aerosol precursors and other gaseous species that may influence the aerosol composition usually change abruptly at the land-sea boundary. Consequently, at either side of the shoreline the aerosol composition will change due to exposure to different sources, the gradual removal of aerosols from sources that abruptly cease to exist, and the injection of a relatively large amount of sea spray over the surf zone.

In the case of an offshore wind, for instance, the very local surf source at the coast line changes the aerosol composition in the lower layers near the surface instantaneously from a continental aerosol to a mixture of continental and surf-generated sea spray aerosol. The relative contribution of both aerosol types depends on the concentrations advected from land and on the source strength and dispersion of the surf-produced aerosol. This mixture is gradually removed due to deposition and other processes. Since the removal processes are size-dependent [e.g., *Slinn and Slinn*, 1980], not only the concentrations will change but also the size distributions. At the same time, at wind speeds exceeding 3–4 m $s^{-1}$, sea spray is produced in response to wave breaking (and thus the developing wave field [e.g., *Monahan and O'Muircheartaigh*, 1986]) and dispersed into the boundary layer. This mechanism compensates, at least in part, for the loss of surf-produced sea spray particles.

Also, as regards the effects of aerosols, the coastal environment has its own specific problems. The mixing of continental and marine aerosol, evolving with fetch, is an important factor for the assessment of observation systems using visible or IR detection [e.g., *Fairall et al.*, 1984; *Gathman*, 1989]. Their performance depends on the transmission of the electromagnetic

[1]Now at Environment Institute, Joint Research Centre, Ispra, Italy.



Paper number 2000JD000025.
0148-0227/01/2000JD000025$09.00

radiation in the atmosphere, which, in turn, is reduced due to extinction by aerosols in the propagation path. Another important application is the effect of sea spray aerosol on coastal ecosystems. In onshore winds, large amounts of sea spray aerosol are advected across the coastline and are deposited close to the coast, where they strongly affect the soil composition and thus maintain the delicate balance that favors the specific coastal vegetation [*Vertegaal*, 1998]. A recent study indicates the large impact of surf-generated aerosols, in comparison with sea-salt aerosol advected from the open sea [*De Leeuw and Moerman*, 1999]. However, also further inland the effects of sea spray cannot be totally ignored, e.g., because of the impact of sea-salt aerosols on corrosion of materials such as buildings and monuments. In offshore winds the surf-produced aerosol offers a large surface area for heterogeneous reactions, such as the uptake of nitric acid ($HNO_3$) by sea spray.

Various models were developed to study the evolution of aerosol size distributions in the marine boundary layer; see *Gong et al.* [1997] for an overview. The model of *Gong et al.* [1997] describes the relevant processes of surface generation of sea spray, vertical transport by diffusion and convection, gravitational settling, dry deposition, and wet removal processes by both in-cloud and below-cloud scavenging. In addition to these processes, the *Fitzgerald et al.* [1998a] model describes aerosol containing sea salt, insoluble continental and sulphuric acid-water particles. Nucleation, coagulation, condensation, in-cloud $SO_2$ oxidation, and exchange with the free troposphere are included, as well as gases participating in the sulphur cycle, such as DMS, $SO_2$, and $H_2SO_4$. An important aspect of this model is the capability to simulate the transport of aerosols in an atmosphere with relative humidity gradients without numerical diffusion. The influence of sources and sinks of sea spray and $H_2SO_4/H_2O$ particles in the marine boundary layer (MBL) has been studied by *Katoshevski et al.* [1999] using a box model.

The coastal aerosol transport (CAT) model, presented in this contribution, was developed to evaluate the importance of sea spray production in the surf zone [*Vignati et al.*, 1998; *Vignati*, 1999]. A simple approach was chosen to evaluate the effects of the surf-produced particles on the physical and chemical properties of coastal aerosols.

## 2. Coastal Aerosol Transport Model (CAT)

CAT is a one-dimensional sectional model that describes the evolution of particle size distributions and aerosol chemical composition in the coastal atmosphere. Only clear sky conditions are treated in the present study and thus such processes as in-cloud transformation and wet deposition are not included in CAT. For the short timescales and aerosol concentrations considered in the present applications, coagulation has no significant influence on the evolution of the particle size distributions. Likewise, effects of entrainment, i.e., exchange of aerosols or gases across the top of the boundary layer, are not accounted for because only at longer timescales do coagulation and exchange with the free troposphere become important [*Fitzgerald et al.*, 1998a].

CAT is initialized at the coastline with a continental particle size distribution, to which the surf aerosol is added. The relevant processes are described in terms of the particle dry radius, to avoid numerical problems due to growth effects in an environment with humidity gradients [*Fitzgerald et al.*, 1998a].

### 2.1. Governing Equation

The general dynamics equation which governs the evolution of the aerosol size distribution $n(r)$ ($r$ is particle radius; in the equations below $n(r)$ is simply written as $n$) can be written as [see, e.g., *Friedlander*, 1977]

$$\frac{\partial n}{\partial t} + \nabla \cdot (\mathbf{v}n) = \nabla \cdot (K \nabla n) + \left(\frac{\partial n}{\partial t}\right)_{\text{cond/evap}} + \left(\frac{\partial n}{\partial t}\right)_{\text{coag}} + \frac{\partial}{\partial z}(v_g n) + \left(\frac{\partial n}{\partial t}\right)_{\text{source/sink}}, \quad (1)$$

where

- $\mathbf{v}$ fluid velocity;
- $K$ eddy diffusivity coefficient;
- $v_g$ particle gravitational settling velocity;
- $z$ height above the surface.

The terms $\nabla \cdot (\mathbf{v}n)$ and $\nabla \cdot (K \nabla n)$ represent advection and turbulent diffusion. In CAT the advection term is set to zero, and the diffusion term in (1) describes only vertical turbulent mixing. The term $(\partial n/\partial t)_{\text{cond/evap}}$ describes the rate of change of the aerosol size distribution due to condensation or evaporation, $(\partial n/\partial t)_{\text{coag}}$ accounts for coagulation, $(\partial n/\partial t)_{\text{source/sink}}$ is the rate of change due to nucleation, emission, and removal, and $\partial/\partial z(v_g n)$ describes gravitational settling.

CAT accounts for the dependence of aerosol processes on meteorological parameters such as wind speed, relative humidity, air temperature or micrometeorological parameters, the values of which can be obtained from measurements or meteorological models. In the simulations presented in this paper, their values are fixed, i.e., horizontal gradients are zero. Vertical profiles of relative humidity and temperature were parameterized [*Vignati*, 1999], and for wind speed vertical variations were neglected.

Nucleation and coagulation are not accounted for in CAT. Nucleation is mainly important in very clean environments. In polluted areas the available aerosol surface promotes condensation, thus leaving little material for nucleation. The continuity equation (1) is solved numerically, as described and tested for aerosol processes by *Vignati* [1999].

### 2.2. Description of Aerosol Properties

The aerosol is described as an external mixture of continental and sea spray particles. Each component is characterized by a discrete size distribution with 26 classes ranging from 0.04 to 12.59 $\mu$m dry radius. The geometrical mean radius of each class is given by $r_I = 0.001 \times 10^{(I+15)/10)}$, $I = 1 - 26$. The choice of the extremes of the interval is determined by the selection of the parameterizations for the thermodynamic parameters used in the model and covers the range of aerosol sizes important in the coastal zone.

The sea spray aerosol, represented in the model by sodium chloride, is composed of particles that are produced both from waves breaking in the surf zone, and from waves breaking on the open sea. The continental component, consisting of a variety of chemical constituents, is represented by ammonium sulphate ($(NH_4)_2SO_4$). The continental and marine components are treated separately, to account for the differences in thermodynamic and microphysical properties of sea salt and ammonium sulphate (see section 3.5), and their consequences for the various processes.

The aerosol is distributed over an air column divided into 10

vertical layers. In each layer the particle concentration is homogeneous. The layer thicknesses increase logarithmically with height to allow for a finer resolution close to the ground where the surface has a relatively large effect on the particle populations and the vertical gradient is largest. The column is advected along a horizontal path, with the speed of the wind.

The time evolution of the particle concentrations $N_{\text{type,I}}$ in class I (type equal to 1 for continental particles and type equal to 2 for sea spray) in the generic layer $L$ is described by the discretized form of equation (1). Equation (1) is written as a function of the dry particle radius. However, the effects of processes that depend on particle radius are calculated with the wet sizes, i.e., for the particles in equilibrium with ambient relative humidity.

## 3. Description of Processes Included in CAT

### 3.1. Sea Spray Production by Breaking Wind Waves

Sea spray aerosol is produced as film and jet droplets when bubbles, entrained in the water by breaking waves, disrupt the sea surface [e.g., *Blanchard*, 1983], and at wind speeds exceeding about 9 m $s^{-1}$, by direct disruption of the wave tops (spume droplets) [*Monahan et al.*, 1983]. The surface flux of sea spray aerosol, i.e., the number of droplets produced per unit surface area and per unit of time is described by the source function. *Andreas* [1998] presented an overview of various source functions. The two most commonly used source functions were derived by *Monahan et al.* [1986] (hereinafter referred to as M86) and by *Smith et al.* [1993] (referred to as S93).

The M86 source function is based on laboratory measurements of the amount of sea-salt droplets produced from an artificially generated breaking wave, expressed as the droplet flux per unit whitecap, and field observations of whitecap cover as a function of wind speed:

$$\frac{dF}{dr} = 1.373U_{10}^{3.41}r^{-3}(1 + 0.057r^{1.05}) \times 10^{1.19e^{-B^2}}, \quad (2)$$

where $U_{10}$ is the wind speed in m $s^{-1}$ at a height of 10 m, $B = (0.380 - \log r)/0.650$, and $dF/dr$ is given in $m^{-2}$ $\mu m^{-1}$ $s^{-1}$. A second mode was added to describe the spume droplet flux. However, application of the latter in models describing effects of sea spray aerosols does not give realistic results [e.g., *Burk*, 1984; *Stramska*, 1987; *Andreas*, 1990a; *Smith et al.*, 1990]. M86 (p. 173) explicitly mention that "the short-comings of their equation as a description of the spume droplet production term are such that its use is not recommended." Therefore the spume droplet contribution as described by M86 is not considered in this work.

S93 derived a sea spray source function from field measurements, using a budget method that considers the atmospheric concentrations as the result of the balance between surface production and removal. This aerosol source function contains contributions from both bubble-mediated droplet production and spume droplets:

$$\frac{dF}{dr_{80}} = \sum_{i=1,2} A_i \exp\left[-f_i\left(\ln\frac{r_{80}}{r_{0i}}\right)^2\right], \quad (3)$$

where $f_I$ and $r_{0I}$ are constants ($f_1 = 3.1, f_2 = 3.3, r_{01} = 2.1$ $\mu$m, and $r_{02} = 9.2$ $\mu$m), $r_{80}$ is the particle radius at 80% relative humidity, and the amplitudes $A_i$ are wind speed dependent coefficients given by

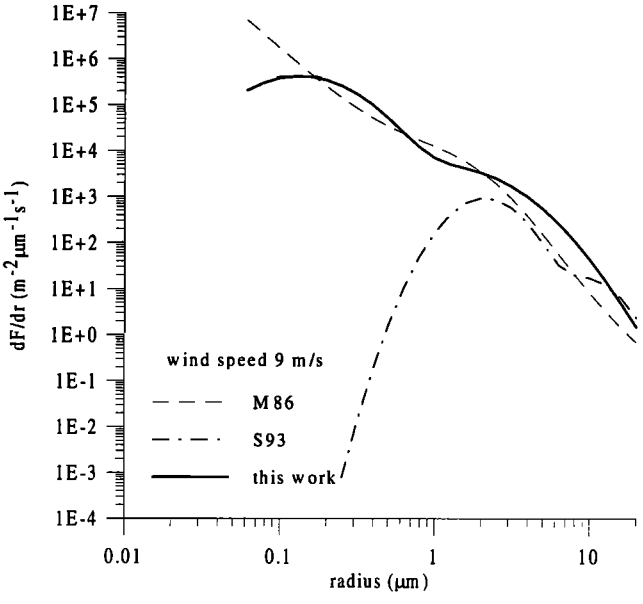


**Figure 1.** Sea spray aerosol source functions $dF/dr$, as a function of radius, for wind speed of 9 m $s^{-1}$.

$$\log(A_1) = 0.0676U + 2.43$$
$$\log(A_2) = 0.959U^{1/2} - 1.476, \quad (4)$$

where $U$ is the wind speed. These relations were obtained from aerosol particle size distributions and meteorological parameters measured at a height of 10 m above the beach, approximately 14 m above mean sea level. $DF/dr_{80}$ is given in $m^{-2}$ $\mu m^{-1}$ $s^{-1}$, and $U$ is given in m $s^{-1}$. Equation (3) is valid for actual radii of up to 20 $\mu$m (at 80% relative humidity), corresponding to a dry radius of approximately 10 $\mu$m.

The M86 and S93 source functions are shown in Figure 1 for a wind speed of 9 m $s^{-1}$. They are similar for particles with radii between 4 and 8 $\mu$m. For larger particles, S93 provides higher fluxes; for smaller particles the curves diverge rapidly. Comparison with surf zone source functions indicates that M86 applies better for smaller particles, whereas S93 appears to better describe the larger particles [*De Leeuw et al.*, 2000a], which supports arguments presented by *Andreas* [1998] concerning the application of M86 and S93. However, comparison with experimental data will show (see below) that simulations using M86 overestimate the concentrations of the smallest particles.

Therefore a practical solution has been sought in the form of an effective source function based on data presented by *O'Dowd et al.* [1997] (this source function is further referred to as OD97). These measurements were made on a ship on the North Atlantic, where coastal effects have no influence. CAT was used to iterate the source function until the data presented in OD97 were reasonably well reproduced. The resulting source function is a sum of three lognormal distributions with parameters given in Table 1. Figure 1 shows that OD97 is in good agreement with M86 for particles with radii larger than 0.1–0.2 $\mu$m, and with S93 for particles larger than about 10 $\mu$m. OD97 applies to a relative humidity of 80%, and for the wind speeds for which data are available (6–17 m $s^{-1}$). In the applications of CAT presented in section 5, the OD97 source function is used.

**Table 1.** Effective Source Function Used in CAT, OD97, Is Formulated as the Sum of Three Lognormal Distributions[a]

| Number $N$, $cm^{-3}$ | Radius $R$, $\mu m$ | Standard Deviation $\sigma$ |
|---|---|---|
| $10^{(0\ 095U+0.283)}$ | 0.2 | 1.9 |
| $10^{(0\ 0422U+0\ 288)}$ | 2 | 2 |
| $10^{(0\ 069U-3\ 5)}$ | 12 | 3 |

[a] $F(\log r) = N/\sqrt{2\pi}\log\sigma\exp(-(\log r - \log R)^2/2\log^2\sigma)$, where $r$ is the particle radius. The geometric mean radius $R$ applies for RH equal to 80%; $U$ is the wind speed in m $s^{-1}$.

### 3.2. Turbulent Mixing

Vertical transport of aerosol particles due to turbulence is parameterized by an eddy diffusivity formulation. The rate of change of the particle number concentration is given by

$$\left(\frac{\partial n}{\partial t}\right) = \frac{\partial}{\partial z}\left(K_z\frac{\partial n}{\partial z}\right). \tag{5}$$

The diffusivity coefficient $K_z$ is assumed to vary with height in the surface layer according to [cf. *Stull*, 1988]

$$K_z = \frac{\kappa u* z}{\phi(z/L)}, \tag{6}$$

where $\kappa$ is the von Karman constant ($\kappa = 0.4$), $u*$ is the friction velocity, and $\phi(z/L)$ is a stability correction given by

$$\phi(z/L) = \begin{cases} 1 + 4.7\ z/L & z/L > 0 \quad \text{stable} \\ 1 & z/L = 0 \quad \text{neutral} \\ (1 - 15\ z/L)^{-1/4} & z/L < 0 \quad \text{unstable.} \end{cases} \tag{7}$$

Above the surface layer the diffusivity coefficient is assumed to be constant throughout the boundary layer, and in the top layer it decreases to zero [cf. *Seinfeld and Pandis*, 1998]. The height of the surface layer was set to 50 m. The height of the boundary layer was in the presented simulations set to either 260 or 1000 m, but observed values can be substituted for actual conditions.

The surface layer expression for the diffusivity coefficient (equation (6)) derives from Monin-Obhukov similarity theory which does not strictly apply in the coastal zone because the sudden land-sea transition leads to a nonequilibrium situation which violates the basic assumptions. However, observations of temperature and humidity profiles at the North Sea near the coast, in offshore wind with often very stable thermal stratification, compare quite well with model predictions based on Monin-Obhukov similarity theory [*De Leeuw and Neele*, 1994]. Similarly, observations of optical turbulence over coastal waters show discrepancies with theoretical predictions, particularly in stable conditions, but in other conditions the predictions are quite reasonable [*Frederickson et al.*, 2001]. These observations justify the use of equation (7), although the results must be critically interpreted. To the best of our knowledge, no other formulations than those based on Monin-Obhukov similarity theory are presently available.

### 3.3. Gravitational Settling

Owing to gravitation, a spherical particle with density $\rho_p$ and radius $r$ falls with a characteristic velocity, the settling velocity $v_g$, given by

$$v_g = \frac{2\rho_p g r^2 C_c}{9\eta}, \tag{8}$$

where $g$ is the gravitational constant, $\eta$ is the dynamic viscosity of air, and $C_c$ is the Cunningham coefficient given by

$$C_c = 1 + \frac{\lambda}{r}[1.257 + 0.4\exp(-1.1r/\lambda)], \tag{9}$$

where $\lambda$ is the mean free path. Equation (9) shows that the settling velocity is a nonlinear function of particle size.

### 3.4. Dry Deposition

Dry deposition is usually described as the results of three processes [e.g., *Slinn and Slinn*, 1980], i.e., transport in the surface layer, transport in the very thin quasi-laminar layer adjacent to the surface, and the actual uptake by the surface. Surface layer transport is described by aerodynamic processes due to turbulence and gravitational settling. In the quasi-laminar layer, no turbulence occurs, and the air is stagnant. Thus transport takes place by Brownian motion and gravitational settling.

The deposition velocity over water is commonly parameterized using an application of the resistance method to a two-layer model proposed by *Slinn and Slinn* [1980]:

$$\frac{1}{v_d} = \frac{1}{k'_c + v_g(r_d)} + \frac{1}{k'_D + v_g(r_w)} - \frac{v_g(r_d)}{[k'_C + v_g(r_d)][k'_D + v_g(r_w)]}, \tag{10}$$

where the first and the second term of the left-hand side of the equation are the resistances in the constant flux layer and in the deposition layer, respectively, with

$$k'_D = \frac{1}{\kappa} C_D U(Sc^{-1/2} + 10^{-3/St}) \tag{11}$$

$$k'_C = \frac{1}{(1-\kappa)} C_D U, \tag{12}$$

where $C_D$ is the drag coefficient, $\kappa$ is von Karman's constant, $U$ is the wind speed, $Sc$ is the Schmidt number defined as the ratio between the kinematic viscosity and the particle diffusivity, $r_d$ and $r_w$ are the dry and wet radii, respectively, $St$ is the Stokes number:

$$St = \frac{v_g u_*^2}{g\nu}, \tag{13}$$

and $\nu$ is the kinematic viscosity of air.

Deposition velocities of submicrometer particles are determined by turbulence, which can easily keep them in suspension due to their small size. For particles larger than 10 $\mu m$ the gravitational effect is dominant, and the dependence of deposition velocity on wind speed vanishes. Because the actual particle size is determined by the chemical composition, the deposition velocity is different for the two populations that are considered in CAT.

### 3.5. Condensation and Evaporation

The equilibrium of a solution droplet with the ambient relative humidity (RH) is described by the Kelvin equation [*Pruppacher and Klett*, 1997]:

$$S = a_w \exp\left(\frac{2M_w\sigma}{RT\rho_w r}\right), \quad (14)$$

where

$S$ saturation ratio, equal to RH/100;
$\sigma$ surface tension of the droplet;
$M_w$ molecular weight of water;
$\rho_w$ density of water;
$a_w$ water activity;
$T$ ambient temperature;
$R$ universal gas constant, equal to 0.08204 L atm $K^{-1}$ $mol^{-1}$.

Water activity and surface tension depend on the particle chemical composition. In CAT the water activity for sodium chloride and ammonium sulphate as function of solute concentration are calculated using data from *Low* [1969]. The surface tension of an electrolyte solution is calculated using an empirical relation [*Pruppacher and Klett*, 1997]. The use of these data is described in detail by *Vignati* [1999].

Two opposing effects control the relationship between the particle size and the saturation ratio. The Kelvin effect, represented by the exponential term in equation (14), tends to increase the vapor pressure when the particle size decreases, while on the other hand the solute reduces the vapor pressure. The latter process is described by Raoult's law.

Equation (14) is used also to derive the source function $F_o$ of dry sea spray particles from the flux $F$ of sea spray at 80% RH:

$$\frac{dF_o}{dr_d} = \frac{dr_{80}}{dr_d}\frac{dF}{dr_{80}}, \quad (15)$$

where $r_d$ is the dry radius. The relation between $r_{80}$ and $r_d$ can be derived from (14); for sodium chloride this results in

$$r_{80} = 1.98894 r_d^{1.00169}. \quad (16)$$

For practical applications, $r_{80} = 2r_d$. It is noted that effects of other chemical components, and in particular organic material that is often present in sea spray, would change this result.

The times required for particles of various sizes to reach thermodynamic equilibrium are presented by *Andreas* [1990b]. The equilibration time of sea spray particles, i.e., the time required to be in equilibrium with ambient relative humidity, is longer than for ammonium sulphate particles [*Fitzgerald et al.*, 1998b]. The time step used in the model is chosen to ascertain that enough time is available to reach the equilibrium size of all particles in each layer. The characteristic time for a sea-salt particle emitted at the sea surface with an initial wet radius of 50 $\mu$m to reach its equilibrium size at 97.5% relative humidity is 150 s. This upper limit implies that particles with a wet radius larger than 50 $\mu$m cannot be included in the model. The corresponding dry particle radius is about 12.5 $\mu$m, large enough to ensure that the majority of the particles of interest for processes involving sea spray aerosol are included. For RH < 97.5%, shorter time steps are used.

## 4. Model Performance: Comparisons With Experimental Data

CAT was tested by comparisons with experimental data. Comparisons were made for various fetches. Where a long fetch is indicated, the model was run for 300 km. Although strictly the assumptions may not apply for such long fetches (or long run times), these tests are mainly to check on the model performance as regards reproducing reasonable size distributions and their wind speed dependence, mainly for particles that are less dependent on processes not included in CAT.

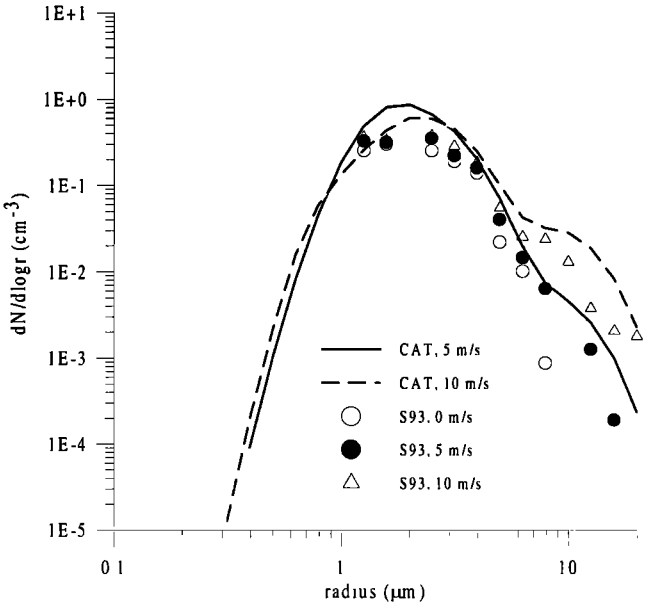


**Figure 2.** Comparison of model results with measurements reported by *Smith et al.* [1993].

### 4.1. Size Distributions

The first test was a comparison of size distributions calculated with the model at a long fetch, at wind speeds of 5 and 10 m $s^{-1}$, with measurements reported by *Smith et al.* [1993]. The measurements were made at the island of South Uist situated approximately 100 km off the northwest coast of the Scottish mainland, with optical particle counters mounted close to the high water mark at a height of 10 m above the beach, i.e., 14 m above the water surface. As described by Smith et al., the data were not influenced by local effects and are representative of the open sea. Results for wind speeds of 0, 5, and 10 m $s^{-1}$, binned in intervals with a width of 1 m $s^{-1}$ (Figure 1 of Smith et al.), are reproduced in Figure 2, together with particle size distributions calculated using CAT. The model results and the Smith et al. data compare favorably.

Having established that the model runs well for particle size distributions measured in the same area as for which the S93 source function was developed, a second test was made using all three source functions to reproduce data presented by *O'Dowd et al.* [1997]. The results presented in Figure 3 show that the simulated particle size distributions at long fetch with each of the source functions compare favorably with the data from *O'Dowd et al.* [1997] at the large particle end. As expected, the S93 source function fails for particles smaller than 2–3 $\mu$m, but the particle size distributions calculated using the M86 source function give excellent results down to about 0.2 $\mu$m. Obviously, the OD97 source function reproduces the particle size distribution over the whole range down to 0.07 $\mu$m.

### 4.2. Wind Speed Dependence

The next test concerns the variation of the aerosol mass concentration with wind speed. CAT was initialized with zero

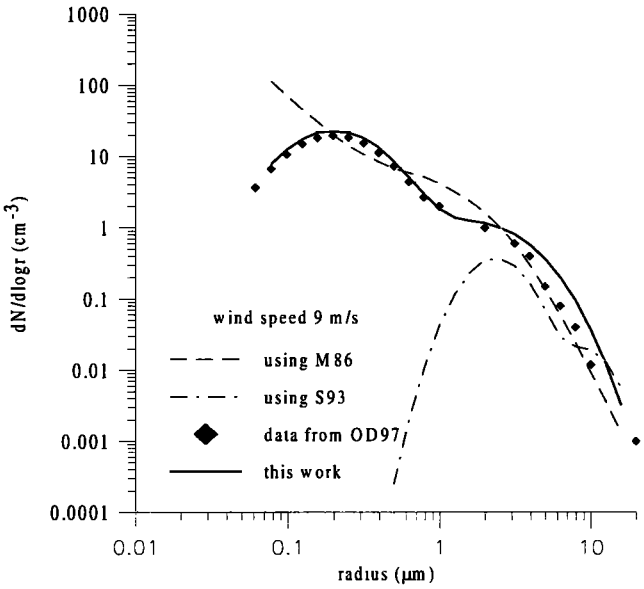


**Figure 3.** Comparison of modeled particle size distributions with data from *O'Dowd et al.* [1997] for a wind speed of 9 m $s^{-1}$. The data were calculated with different source functions.

aerosol concentrations, and the only aerosol source was surface-generated sea spray. The concentrations were evaluated for various wind speeds, with neutral thermal stratification and well-mixed water vapor concentrations, over a long fetch. At the end of the runs the total sea spray aerosol mass was evaluated from the particle size distributions at a height of 10 m above the sea surface. The calculations were made using M86 and S93. Results are presented in Table 2, where the coefficients are given for power law fits to the aerosol mass versus wind speed relations ($\ln c = \ln b + a U$). The results are compared with parameterizations published by *Gong et al.* [1997], based on results from *Exton et al.* [1986], derived from aerosol size distributions measured at the coast of the Hebrides (Scotland), and from *Marks* [1990], measured on Meetpost Noordwijk, an offshore tower in the North Sea at 9 km from the Dutch coast. The wind speed dependence derived from the CAT calculations is in good agreement with the results from Exton et al. This similarity was to be expected because the source function of *Smith et al.* [1993] used in the model was derived from aerosol data collected at the same site, but from a different data set.

### 4.3. Aerosol Transport: Evolution of Surf Plume

A qualitative test of the model was obtained from a comparison with data from an experiment in Duck, North Carolina (United States), in February 1998. Horizontal and vertical profiles of aerosol backscatter coefficients over the surf and further out to 3 km offshore were measured with the LIDAR of the Naval Research Laboratory (NRL) in Washington, D. C. [*Hooper et al.*, 1996] (see also http://wvms.nrl.navy.mil/7221/vil.html). Data from a previous LIDAR experiment at this site [*Hooper and Martin*, 1999] compare favorably with the results from the EOPACE surf measurements on the California coast [*De Leeuw et al.*, 2000a] shown in Figure 4. Based on this similarity, the EOPACE data were used as input for CAT for an independent simulation to test the model versus the LIDAR measurements.

**Table 2.** Dependence of Sea-Salt Mass Concentrations on Wind Speed ($\ln c = \ln b + aU$): Results From CAT Using M86 and S93, and Comparison With Experimental Data

| Reference | Maximum Wind, m $s^{-1}$ | $a$, s $m^{-1}$ | $b$, μg $m^{-3}$ |
|---|---|---|---|
| *Exton et al.* [1986] | 20 | 0.17 | 14.3 |
| *Marks* [1990] | 24 | 0.23 | 1.13 |
| CAT, using S93 | ... | 0.17 | 3.9 |
| CAT, using M86 | ... | 0.14 | 8.1 |

An example of a lidar scan of aerosol backscatter by plumes produced over the surf and transported out over the ocean by an offshore wind is shown in Figure 5a (W. A. Hooper, private communication, 1999). The backscatter levels have been set such that signals from ambient aerosols are masked and only the surf-produced plumes are shown. The plumes grow with distance from the beach, to heights of about 100 m after 600 m, while the backscatter intensity decreases due to dilution of the aerosol concentrations by dispersion. Operation of the LIDAR in a different mode, allowing for visualization of the plumes over much larger distances, confirms that the plumes continue to grow with fetch. Figure 5a also shows backscatter from a height of about 200 m, suggesting that this is the cloud layer. Hence it is anticipated that the boundary layer height for this day was about 200 m.

A simulation was made with CAT, using the meteorological parameters measured during the experiment, for very short fetch to reproduce these data. Results are shown in Figure 5b, as a contour plot of the aerosol surface area (as a measure of the aerosol backscatter coefficient). The development of the aerosol plumes and the diminishing concentrations with increasing distance from the coast are similar to those measured with the LIDAR. The initial plume heights in Figure 5b are higher than in the LIDAR data. This is due to the initialization of CAT with the EOPACE data that were measured on the beach at an average distance of 75 m from the water line, where the plume heights were somewhat higher than immediately over the surf. The growth of about 40 m over a distance of 500 m observed with the LIDAR (Figure 5a) is similar to that shown in Figure 5b for the 20 $\mu m^2$ $cm^{-3}$ contour line. Also, the variation of particle concentrations, at a certain height, with distance from the coastline is well reproduced by CAT.

The similarity between the aerosol plumes calculated with CAT and those observed with the NRL LIDAR in Duck suggests that CAT provides a reasonable description of the aerosol transported over a short distance by offshore winds. Qualitatively, both the vertical dispersion and the dilution with distance are well reproduced.

## 5. Applications

CAT was used to determine to what extent the effect of surf-produced sea spray must be taken into account for the description of various processes. The simulations were made for fetches up to 25 km, and for wind speeds up to 8 m $s^{-1}$, the highest wind speed for which surf data are available [*De Leeuw et al.*, 2000a]. Studies were made of (1) the contribution of surf-produced sea spray aerosol to the total concentrations including surface production by breaking waves, (2) the mixing

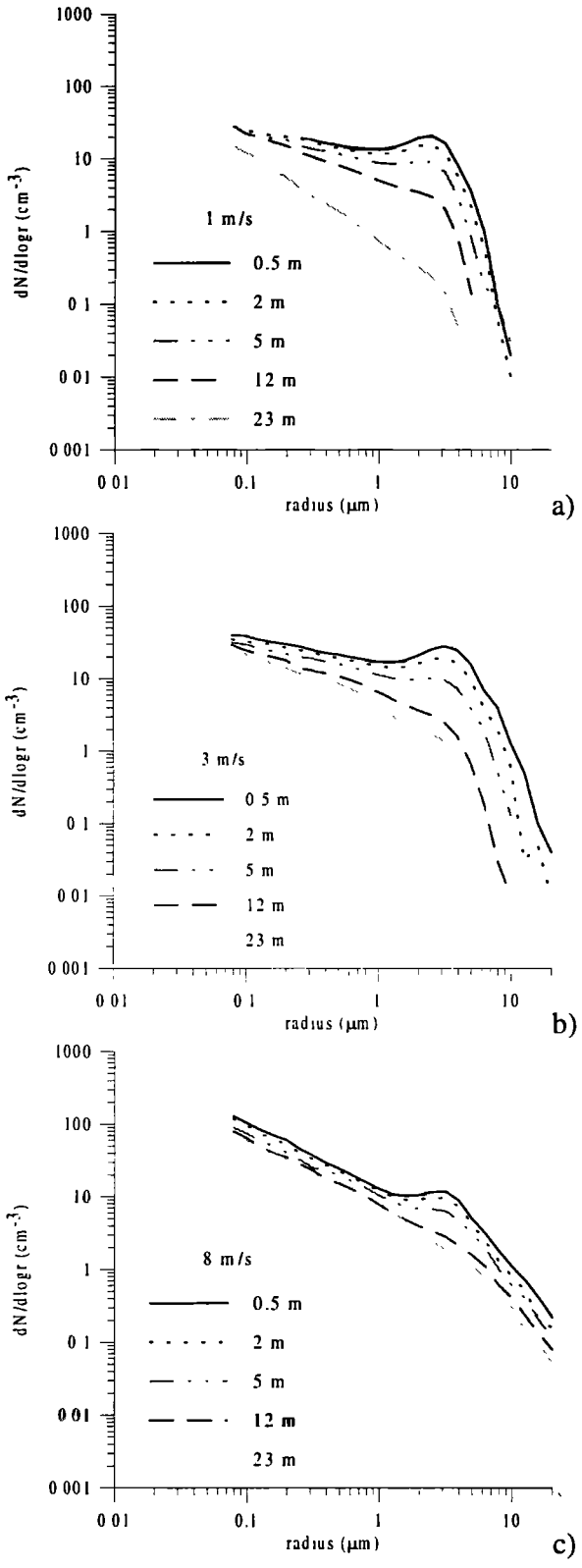


**Figure 4.** Mean initial sea spray size distributions over the surf for (a) 1, (b) 3, and (c) 8 m $s^{-1}$. The levels are identified by their mean height.

of sea spray aerosol and continental aerosol, and (3) the heterogeneous reaction between sea-salt aerosol and nitric acid and the evolution of aerosol and nitric acid profiles with fetch. In all cases, the sea spray population was initialized with the EOPACE experimental data for the size distributions and vertical profiles of surf-produced aerosol (see Figure 4).

### 5.1. Horizontal Transport and Effect on Sea Spray Concentrations

The contribution of surf-produced aerosols to the sea spray size distributions in offshore winds was simulated for wind speeds of 1 and 8 m $s^{-1}$. Only surf-produced aerosol and production at the sea surface were considered. Continental backgrounds were set to zero. The computations were made for a column with a thickness of 260 m, which is representative for the marine boundary layer height off the California coast. Particle size distributions calculated for different fetches are presented in Figure 6. Initially, the concentrations are decreasing fast for all sizes. For the smaller particles the concentrations at a fetch of 25 km are about 1 order of magnitude smaller than the original values. As can be seen from (10)–(12), the removal rate is wind speed dependent, with higher deposition velocities for larger wind speed.

The removal of particles larger than 1 μm is partially balanced by surface production. At the lowest wind speed, obviously no primary production occurs. The effect of surface production at 8 m $s^{-1}$ is clear from a comparison of Figures 6a and 6b. Where at the lower wind speed the concentrations of particles larger than 2–3 μm decrease very rapidly, the primary production at the higher wind speed appears to sustain the concentrations at the largest fetches.

This is further illustrated with the results presented in Figure 7 for 8 m $s^{-1}$, where concentrations of particles in the layer centered around 12 m are plotted as a function of the distance from the coastline for two situations. One set of curves shows a simulation of the evolution of the concentrations of the surf-produced particles with fetch, in the absence of surface production. For the calculation of the other set of curves, the concentrations over the surf were set to zero, and the evolution of the sea spray concentrations due to primary production was calculated. Obviously, the concentrations of the surf-produced particles decrease with fetch, fastest for the largest particles due to removal by dry deposition. Also as expected, the concentrations of the surf-produced particles increase. However, the rate of increase is determined by the balance between production and removal, and is faster for the 0.5 μm particles than for the larger ones. For the simulations presented in Figure 7, with the EOPACE surf concentrations and the OD97 source function, this results in a situation where the surf-produced particles provide the largest contribution to the sea spray concentrations to fetches of more than 35 km. As suggested by the results in Figure 6b, two modes develop, roughly around 0.5 and 5 μm, and for these modes the surface production becomes more important only at fetches of 45 and 38 km, respectively. For particles of 10 μm radius this occurs at a fetch of 50 km. Even at this fetch, the concentrations are still increasing for all sizes.

### 5.2. Mixing of Continental and Sea Spray Aerosol

The mixing of continental and sea spray aerosol in offshore winds was studied for fetches up to 100 km, accounting for both surf and surface production of sea spray. The continental aerosol is initialized with a size distribution which represents the average of the size distributions obtained during the EOPACE experiments in La Jolla during offshore winds, and is modeled as the sum of three lognormal size distributions

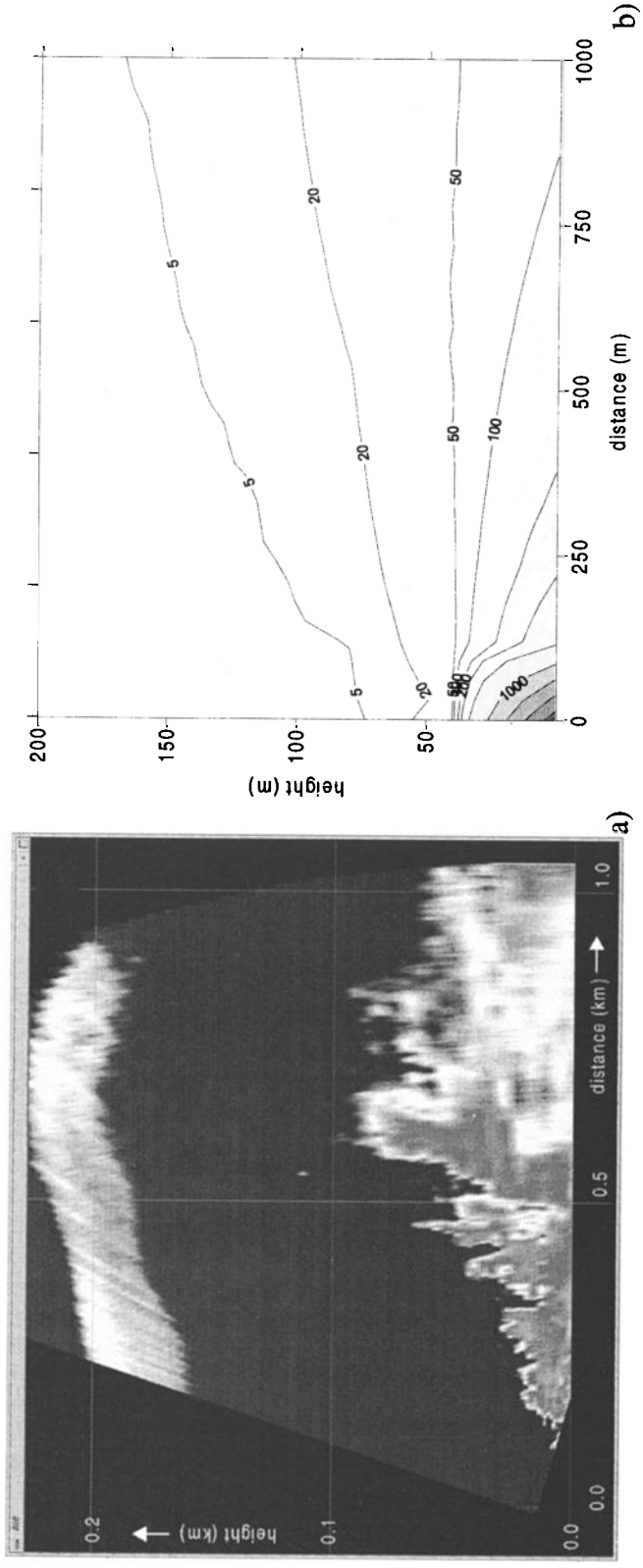


**Figure 5.** Aerosol plumes produced by waves breaking over the surf and transported offshore by the wind. (a) Measurements with a LIDAR system as described in the text (figure made available by W. Hooper from NRL). (b) Contour plot of aerosol surface area concentrations (in $\mu m^2\ cm^{-3}$) calculated with CAT. For easy comparison, the two figures have been scaled such that they have the same horizontal and vertical dimension.

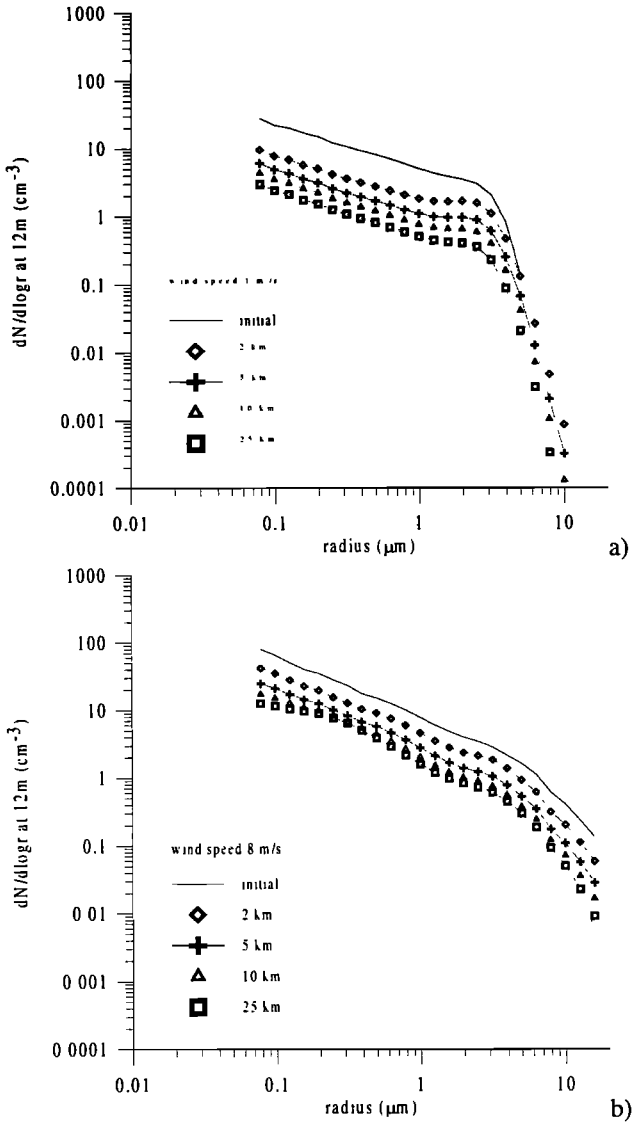


**Figure 6.** Modeled sea spray size distributions at 0, 2, 5, 10, and 25 km from the coastline at 12 m height. Wind speed is (a) 1 and (b) 8 m s$^{-1}$. Initial conditions as shown in Figure 3.

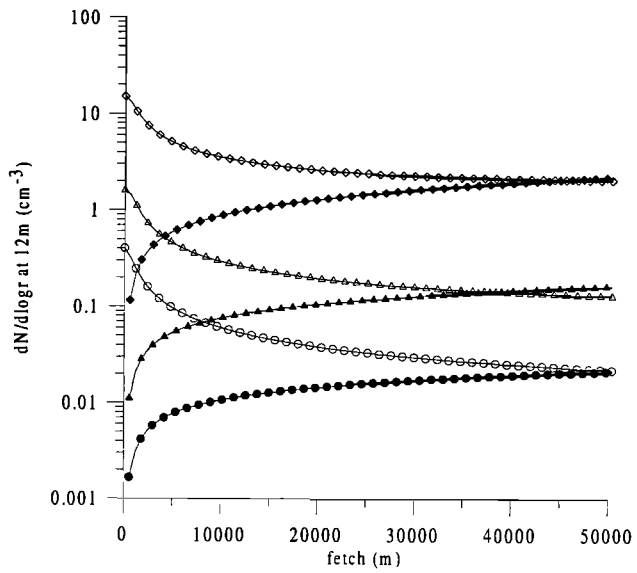


**Figure 7.** Modeled particle concentrations as a function of distance from the coastline for particles of 0.5 (diamonds), 5 (triangles), and 10 (circles) μm at 12 m height. Wind speed is 8 m s$^{-1}$. Initial conditions represented by EOPACE data. Open symbols represent the contribution of the surf-produced particles; solids symbols denote that of the surface-produced particles.

(see Figure 8). It is assumed to be uniformly mixed throughout the boundary layer.

The particle chemical composition at various fetches, i.e., the percentages of the total particle numbers consisting of either sea salt or ammonium sulphate is presented in Table 3 for particles with wet radii of 0.2, 2, and 20 μm. The results apply to calculations at a height of 12 m.

As expected from the overwhelming amount of particles advected from land, as compared to both the surf production and the primary production at sea, the smallest particles ($r$ = 0.2 μm) are mainly ammonium sulphate. Even at low levels over the surf zone, sea-salt particles contribute only 2%. Their contribution decreases rapidly due to redistribution of the particles over the column by diffusion.

Supermicron sea spray particles are produced over the surf zone in relatively much greater quantities, and hence their contribution to the total concentration is much more important. Over the surf the particles with a radius of 2 μm consist of similar amounts of sea salt and continental aerosol. While advected over the sea, effective mixing takes place due to vertical transport, and the concentrations are also influenced by removal by dry deposition and production of sea spray. Thus, initially, the fraction of sea spray decreases due to dilution over the column and then increases again because of the primary production of sea salt and the removal of continental

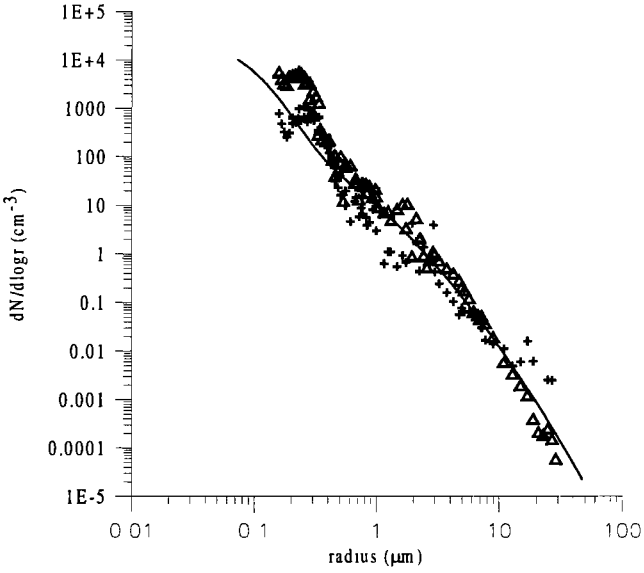


**Figure 8.** Comparison of the lognormal size distributions used in the calculations (line) with experimental data obtained during the EOPACE experiments in La Jolla (triangles and crosses). Two different particle size distributions are shown, with slightly different characteristics, which were both measured in an offshore wind, upwind from the surf zone, and are representative for the aerosol advected from land.

**Table 3.** Contribution of Sea-Salt (SS) and Ammonium Sulphate (AS) Particles to the Total Particle Number Concentrations at 0.2, 2, and 20 $\mu$m Wet Radius at Various Fetches, Calculated With CAT

| | Initial | | at 2 km | | at 25 km | | at 100 km | |
|---|---|---|---|---|---|---|---|---|
| $r$, $\mu$m | SS, % | AS, % | SS, % | AS, % | SS, % | AS, % | SS, % | AS, % |
| 0.2 | 2 | 98 | 1 | 99 | 1 | 99 | 1 | 99 |
| 2 | 51 | 49 | 34 | 66 | 20 | 80 | 26 | 74 |
| 20 | 97 | 3 | 90 | 10 | 63 | 37 | 73 | 27 |

aerosol that is not replaced from any sources. At 25 km the continental component contributes 80% to the total mass in the 2 $\mu$m fraction. The extended simulation shows that at 100 km this contribution is reduced to 74%.

The largest particles (20 $\mu$m) are dominated by sea salt at all fetches from the surf zone up to 100 km. This is explained by the very small initial contribution of continental aerosol to particles of this size, which are effectively removed by gravitational settling and dry deposition. Thus the continental particles disappear relatively fast, while sea spray is efficiently produced at the sea surface.

### 5.3. Interaction Between Nitric Acid and Sea Spray Particles Close to the Coast

Nitric acid ($HNO_3$) is produced from $NO_2$, a gas phase product from combustion processes, at a rate of a few percent per hour. It reacts in the presence of ammonia to form nitrate in the aerosol phase. In the marine atmosphere, $HNO_3$ is removed by reaction with sea-salt aerosol:

$$HNO_3(g) + NaCl(s) \rightarrow NaNO_3(s) + HCl(g). \quad (17)$$

Both $HNO_3(g)$ and $NaNO_3(s)$ are deposited to the sea surface where they contribute to eutrophication. The Cl replacement reaction (17) is important because of the different deposition velocities for gaseous species and particulate matter. Hence also the fluxes of $HNO_3$ are influenced by reaction (17) [*Geernaert et al.*, 1998]. The following simulation is focused on the effect of surf-produced particles on nitric acid profiles. Therefore the production of $HNO_3$ due to dissociation of ammonium nitrate is neglected.

The variation of $HNO_3$ profiles with fetch due to surf-produced particles was evaluated using CAT for a wind speed of 8 m $s^{-1}$. In the calculations, only sea spray particles were considered and no continental aerosol. Both the sea-salt aerosol surface available for condensation of $HNO_3$, and the very $HNO_3$ concentrations change with distance to the coast. Apart from the transformation of $HNO_3$ into the aerosol phase, the gas is also removed by deposition to the water surface. The dry deposition velocity of nitric acid to the sea surface is related to the atmospheric conditions and the sea surface characteristics

$$v_{dHNO_3} = \frac{1}{R_a + R_b + R_s}, \quad (18)$$

where $R_a$ is the aerodynamic resistance, $R_b$ is the resistance of the "quasi-laminar boundary layer" adjacent to the sea surface, and $R_s$ is the surface resistance. The resistances are calculated following *Ganzeveld and Lelieveld* [1995].

The description of the reaction between $HNO_3$ and sea salt in CAT accounts for gas-phase diffusion, interface mass transport, and the rapid aqueous-phase equilibrium between the gas-phase and the dissolved phase. At any relative humidity where particles can be considered dilute solutions, the mass transport can be calculated by assuming the rapid establishment of aqueous-phase equilibria, expressed by Henry's law [*Schwartz*, 1986; *Dentener*, 1993]. The dynamics of species in the gaseous phase can then be described by the following equations:

$$\frac{dp_i}{dt} = \frac{w_L}{H_i} k_m c_i(\text{aq}) - w_L k_m p_i, \quad (19)$$

where $p_i$ is the partial pressure (atm) of the gas phase species $i$, $w_L$ is the aerosol water content (nondimensional), $H_i$ is the effective Henry's law coefficient (mol $L^{-1}$ atm), and $c_i(\text{aq})$ is the concentration of the species $i$ in the water phase (mol $L^{-1}$). The parameter $k_m$ is a transfer coefficient ($s^{-1}$) given by

$$k_m = \left( \frac{r^2}{3D_m} + \frac{4r}{3v_m\alpha} \right)^{-1}, \quad (20)$$

where $D_m$ is the diffusion coefficient of the species in the gas phase, $v_m$ is the average molecular speed, and $\alpha$ is the accommodation coefficient [*Schwartz*, 1986]. The two terms on the right-hand side of the equations describe the gas phase transport and the interfacial mass transport, respectively. The coefficient $k_m$ approaches the correct values both in the continuum and in the kinetic regimes. The time variation of the aqueous phase concentration is given by

$$\frac{dc_i(\text{aq})}{dt} = \frac{1}{RT} k_m p_i - \frac{1}{H_i RT} k_m c_i(\text{aq}), \quad (21)$$

where $R$ is the gas constant, equal to 0.08204 L atm $K^{-1}$ $mol^{-1}$. Accounting for aqueous phase reactions would require an additional term in (21).

The particle pH is accounted for in the calculation of the effective Henry's law coefficient. When the particles become very acidic, the transfer of $HNO_3$ from the gas phase will stop. Only the equations for $HNO_3$-$NO_3^-$ dynamics have been implemented, and the droplet pH decreases as nitric acid condenses.

Results of the simulations, i.e., profiles for sea spray and $HNO_3$ for various fetches, are presented in Figure 9. Initially, the sea spray concentration profile (Figure 9a) shows a large gradient from the surface level to the height of the surf plumes (30 m). After 2 km, the concentrations near the surface have significantly decreased, mainly due to diffusion into the upper layers. With increasing fetch the vertical gradients gradually decrease further, but even at 25 km some vertical variation is still visible in Figure 9a.

The nitric acid profile was initialized with a constant value of 200 ppt (0.5 $\mu$g $m^{-3}$) at the coastline. In the evolution of the gas concentration profile, compare with Figure 9b, the influence of the two competing processes, dry deposition of $HNO_3$

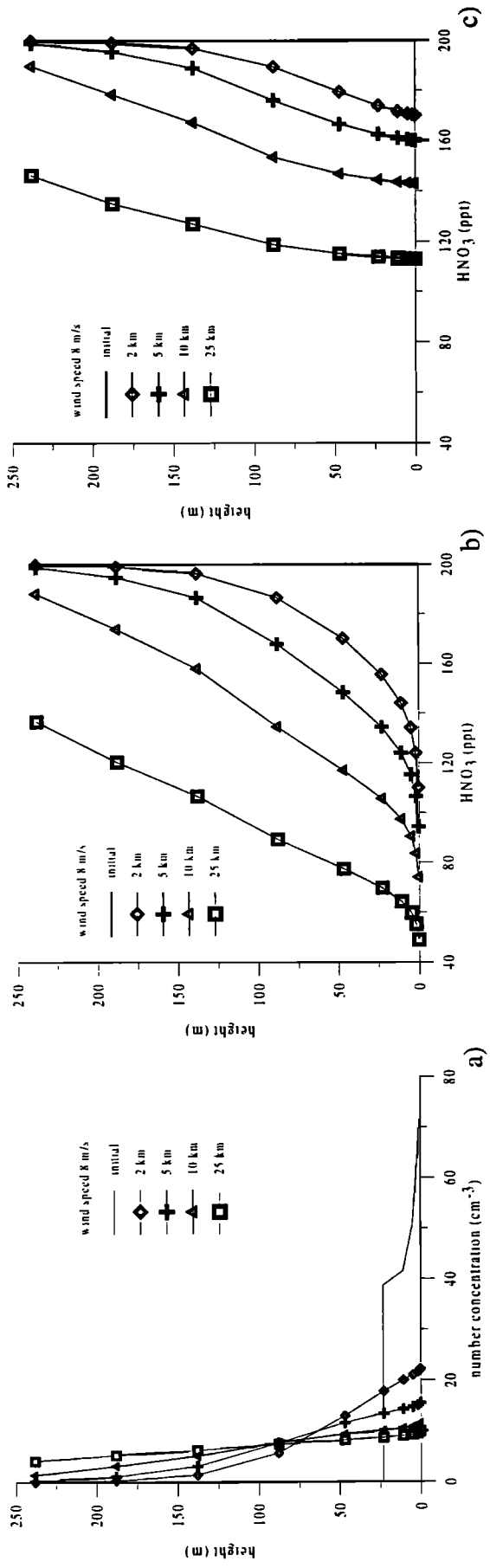


**Figure 9.** Profiles of (a) sea spray particles and (b, c) nitric acid concentrations as function of the distance from the coast. Calculations were made with CAT, using initial conditions in Figure 4; wind speed 8 m s$^{-1}$. The nitric acid profiles in Figure 9b were calculated as described in the text, accounting for both dry deposition of $HNO_3$ to the surface and uptake by sea spray; in Figure 9c the gaseous deposition was set to zero.

and uptake by sea spray aerosols, is evident. Gaseous deposition obviously only takes place in the lowest layer, and the profile is shaped by diffusion between the various layers and uptake by sea spray, which initially occurs only in the lowest layers. As the aerosols are dispersed in the vertical, the sea spray provides a distributed sink throughout the boundary layer. This is best illustrated with a simulation where the gaseous deposition was set to zero (Figure 9c). This figure shows that after 2 km the $HNO_3$ concentrations are significantly reduced near the surface. At higher levels the concentrations become lower as the fetch increases and the sea spray concentrations are more homogeneously distributed over the column. Comparison with the data in Figure 9b, where both effects were taken into account, shows that the initial decrease of the $HNO_3$ concentrations in the lowest layer is mainly due to gaseous deposition, but in the layers above, sea spray becomes increasingly important. Overall, at a fetch of 2 km, about 40% of the $HNO_3$ removal in the lower 20 m is due to uptake by sea-salt particles. The comparison of Figures 9b and 9c also shows that at longer fetches the $HNO_3$ concentrations in the highest layers are mainly determined by the removal due to the uptake by sea spray. Further, in the lowest layer the dry deposition flux is limited by the amount of $HNO_3$ diffusing downward from higher layers, and thus the influence of deposition on the $HNO_3$ concentrations in the column is reduced with respect to the sea-salt effect. At the longest fetch of 25 km, about 80% of the reduction of the $HNO_3$ concentrations in the column is due to the effect of sea spray.

## 6. Discussion

CAT has been developed to evaluate processes in the coastal atmosphere involving aerosols. The simulations were made with continental aerosol, represented by ammonium sulphate, and sea spray, each with their own thermodynamic properties. Obviously, the chemical composition can be chosen according to data applying to a particular site, or based on emission inventories. However, for each compound the thermodynamic properties are different, and thus require proper formulation for inclusion in CAT.

The meteorological parameters used in the presented simulations are simplified. The purpose of the present study is to indicate the importance of various effects, rather than to provide an exact quantitative analysis for a given situation. The latter requires a sophisticated meteorological model describing the coastal meteorology including the values for the various micrometeorological parameters used in CAT at each time step. In addition, the evolution of the wind speed with increasing fetch, and thus the wave field, implies that the wave breaking characteristics are different from those in a well-developed wave field in balance with the wind. This will also have consequences for the sea spray source function. Model results by *Geernaert and Astrup* [2000] indicate that for neutral stratification the wind speed profile and drag coefficient are significantly affected by coastal influences only for fetches smaller than 10 km. Hence also the effect on the source function will be significant at such fetches, where, according to results presented above, the surf-produced aerosol dominates the sea spray concentrations. Thus the influence of the developing wave field on the sea spray concentrations at short fetches is not expected to significantly affect the results of CAT.

This conclusion is based on the dominance of the surf-produced sea spray aerosol, and the question arises whether the surf aerosol source used in CAT, derived from measurements on the California coast, also applies elsewhere. *De Leeuw et al.* [2000a] derived their source function from measurements at two different sites with significantly different surf widths. The results for both sites were similar. CAT results also compare favorably with LIDAR measurements in Duck (North Carolina) on the North Atlantic coast. These observations indicate the general applicability of CAT for oceanic coastal sites.

Insights in the differences between surf aerosol production along the shores of the open Pacific Ocean and along the shores of relatively enclosed seas such as the Baltic and the North Sea are available from *De Leeuw et al.* [2000a, 2000b] and *De Leeuw and Moerman* [1999]. *De Leeuw et al.* [2000a] compared the EOPACE results with data obtained on the Polish coast of the Baltic from *Petelski and Chomka* [1996], after accounting for differences in both measurements and data analysis, as well as factors such as swell and salinity. They concluded that at higher wind speeds the surf production at each location is quite similar. At very low wind speeds, large differences remain due to the absence of swell.

Also, results presented by *De Leeuw and Moerman* [1999] indicate the large contribution of surf-produced aerosols to the sea spray concentrations. Furthermore, LIDAR measurements along the North Sea coast clearly reveal the existence of surf-produced aerosol plumes in offshore winds and their transport over sea over distances of at least 5 km [*De Leeuw et al.*, 2000b].

No ideal data set is presently available that could be used for the validation of CAT, i.e., a data set containing vertical profiles of aerosol particle size distributions as a function of distance from the coast line. A comparison of CAT with available other types of experimental data yields good qualitative results. The particle size distributions calculated with CAT for long fetch compare favorably with data from two different experiments on the North Atlantic [*Smith et al.*, 1993; *O'Dowd et al.*, 1997]. The variation of the aerosol mass with wind speed is reasonably reproduced by CAT, as deduced from comparisons with data sets for the North Atlantic [*Exton et al.*, 1986] and the North Sea [*Marks*, 1990]. The concentrations over the North Sea are lower (see *Gong et al.* [1997] for a discussion of the wind speed dependence observed at various locations). Finally, the evolution of the sea spray aerosol plume produced over the surf zone is well reproduced by CAT.

Having established that CAT reasonably predicts the spectral shape, the concentrations, and their wind speed dependence, as well as aerosol dispersion, the model was applied to several situations to assess the influence of surf-produced sea spray aerosol on processes in the MBL. First, the influence of surf production on the total concentrations of sea spray was investigated for fetches up to 25 km. The results depend on particle size. It is noted that secondary production, which often dominates the accumulation mode aerosol concentrations, is not included in CAT. *O'Dowd et al.* [1997, p. 75] note that "under clean marine conditions and moderate to high winds, the sea-salt aerosol could readily dominate the accumulation mode aerosol." This refers to a wind speed of 17 m $s^{-1}$, which is much higher than the maximum wind speed of 8 m $s^{-1}$ considered in the present work.

The calculations apply for the highest wind speeds considered in this work, 8 m $s^{-1}$. For higher wind speeds the situation may be different, but unfortunately no data are available for the surf source function. This is a limitation, but it is noted that

for many coastal regions a mean wind speed of 8 m $s^{-1}$ is rather high. Hence, in modeling studies of coastal effects involving sea spray aerosol, the effect of production in the surf zone needs to be accounted for.

Similarly, the effect of surf-produced aerosol cannot be neglected for applications in which the aerosol composition is important. Results presented show that at a height of, e.g., 12 m, the sea spray size distribution varies with fetch and that this variation is wind speed dependent. Results in Table 2 show that the contributions of continental and sea spray aerosols to the total aerosol concentrations are size-dependent and in fact the fraction of continental aerosol in certain size ranges may initially increase, due to dilution of the sea spray fraction because of vertical diffusion, before the effect of removal causes a decrease of this fraction.

Finally, an example was presented of the effect of sea spray on flux profiles of nitric acid. In the absence of surf-produced aerosol, there would initially only be gaseous deposition at the sea surface, until enough sea spray would have been produced to have a significant effect. With the high concentrations of sea spray immediately available at the coast line, nitric acid is effectively removed also at very short fetches, thus providing a possible explanation for observed effects in coastal regions as regards aerosol composition [e.g., *Schulz*, 1996]. Estimates for the deposition of $HNO_3$ are usually based on measurements taken on the open ocean. Effects close to the coast line, where they may be largest in view of the vicinity of sources for gaseous species and the large sea spray surface area, were thus far not addressed [*De Leeuw et al.*, 2001]. With a contribution of about 30%, atmospheric transport and dry deposition have been indicated as an important pathway for eutrophication of coastal seas [*North Sea Task Force*, 1993]. Therefore an accurate estimate of the deposition of nitrogen compounds such as $HNO_3$ is important for the evaluation of reduction strategies.

An important aspect of the surf-produced aerosol may be that even at very low wind speeds, where wave breaking and thus production of sea spray does not occur on the surface of the open ocean, the presence of swell still causes wave breaking at the coast line and thus surf production. Thus, even at very low wind speeds, sea spray aerosol is available that offers surface for heterogeneous reactions.

## 7. Conclusions

CAT was developed to study effects of surf-produced aerosols on processes in the coastal marine boundary layer, both over sea and over land. Here only studies were reported in offshore winds, where the surf-produced aerosol is advected over the sea. The surf can be an intensive source of sea spray aerosol. Such effects were either ignored, or avoided when measurements were made at coastal sites.

The present work shows clearly that surf-produced aerosol has a large influence on the sea spray concentrations in the coastal marine atmospheric boundary layer, and thus on the relative contributions of continental and marine aerosol, which in turn is important to assess effects on transmission of electromagnetic radiation and thus the performance of electro-optical systems and visibility. Furthermore, sea spray aerosol is produced in the surf zone in very high concentrations that immediately at the coast line are available for heterogeneous chemical reaction, and thus influences, e.g., atmospheric input of nitrogen in coastal waters.

Hence surf-produced aerosol cannot be ignored and needs to be accounted for both in modeling and in experimental work. A simple assessment of the particle size distribution at either side of the coastline is not sufficient. A transport model such as CAT could be used in the evaluation of processes in the coastal atmospheric boundary layer involving aerosols.

**Acknowledgments.** The work presented in this paper was part of Elisabetta Vignati's Ph.D. work supported by the Danish Research Council (SNF). The work of Gerrit de Leeuw was supported by the Netherlands Ministry of Defence, assignments A95KM729 and A99KM617, and the U.S. Office of Naval Research, grant N00014-96-1-0581. W. A. Hooper from the Naval Research Laboratory in Washington, D. C. (United States) is acknowledged for making available the LIDAR data, and Mike Smith from the University of Leeds (United Kingdom) is acknowledged for valuable discussions and suggestions concerning data used in this work.

## References

Andreas, E. L., Model estimates of the effects of sea spray on air-sea heat fluxes, in *Modeling the Fate and Influence of Marine Spray*, edited by P. G. Mestayer, E. C. Monahan, and P. A. Beetham, pp. 17–28, Mar. Sci. Inst., Univ. of Conn., Avery Point Groton, 1990a.

Andreas, E. L., Time constants for the evolution of sea spray droplets. *Tellus, Ser. B*, *42*, 481–497, 1990b.

Andreas, E. L., A new sea spray generation function for wind speeds up to 32 m $s^{-1}$, *J. Phys. Oceanogr.*, *28*, 2175–2184, 1998.

Blanchard, D. C., The production, distribution, and bacterial enrichment of the sea-salt aerosol, in *Air-Sea Exchange of Gases and Particles*, edited by P. S. Liss and W. G. N. Slinn, pp. 407–454, D. Reidel, Norwell, Mass., 1983.

Burk, S. D., The generation, turbulent transfer and deposition of the sea-salt aerosol, *J. Atmos. Sci.*, *41*, 3040–3051, 1984.

De Leeuw, G., and M. Moerman, Zeezout in de lucht aan de kust bij Voorne: Concentraties en aanvoer door de lucht in relatie tot de meteorologische omstandigheden (in Dutch) report, Minist. van Verkeer en Waterstaat, Dir.-Gen. Rijkswaterstaat, Dir. Zuid-Holland, 1999.

De Leeuw, G., and F. P. Neele, Temperature and humidity profiles over coastal water, in *Proceedings of Second International Conference on Air-Sea Interaction and on Meteorology and Oceanography of the Coastal Zone*, pp. 184–185, Am. Meteorol. Soc., Boston, Mass., 1994.

De Leeuw, G., F. P. Neele, M. Hill, M. H. Smith, and E. Vignati, Production of sea spray aerosol in the surf zone, *J. Geophys. Res.*, *105*, 29,397–29,409, 2000a.

De Leeuw, G., et al., Atmospheric nitrogen inputs into the coastal ecosystem (ANICE) ENV4-CT97-0594: Second annual report (Feb. 1, 1999–Jan. 31, 2000), *Rep. FEL-00-C125*, Phys. and Electron. Lab., Neth. Org. for Appl. Sci. Res., The Hague, Netherlands, 2000b.

De Leeuw, G., et al., Atmospheric input of nitrogen into the North Sea: ANICE project overview, *Nearshore Coastal Oceanogr.*, in press, 2001.

Dentener, F., Heterogeneous chemistry in the troposphere, Ph.D. thesis, Univ. of Utrecht, Utrecht, Netherlands, 1993.

Exton, H. J., J. Latham, P. M. Park, M. H. Smith, and R. R. Allan, The production and dispersal of maritime aerosol, in *Oceanic Whitecaps and Their Role in Air-Sea Exchange Processes*, edited by E. C. Monahan and G. MacNiocaill, pp. 175–193, D. Reidel, Norwell, Mass., 1986.

Fairall, C. W., K. L. Davidson, and G. E. Schacher, Application of a mixed-layer model to aerosols in the marine boundary layer, *Tellus, Ser. B*, *36*, 203–211, 1984.

Fitzgerald, J. W., W. A. Hoppel, and F. Gelbard, A one-dimensional model to simulate multicomponent aerosol dynamics in the marine boundary layer, 1, Model description, *J. Geophys. Res.*, *103*, 16,085–16,102, 1998a.

Fitzgerald, J. W., J. J. Marti, W. A. Hoppel, G. M. Frick, and F. Gelbard, A one-dimensional model to simulate multicomponent aerosol dynamics in the marine boundary layer, 2, Model application, *J. Geophys. Res.*, *103*, 16,103–16,117, 1998b.

Frederickson, P. A., K. L. Davidson, C. R. Zeisse, and C. S. Bendall, Estimating the Refractive Inex Structure Parameter ($C_n^2$) over the ocean using bulk methods, *J. Appl. Meteorol.*, *39*, 1770–1783, 2001.

Friedlander, S. K., *Smoke, Dust and Haze*, 317 pp., John Wiley, New York, 1977.

Ganzeveld, L., and J. Lelieveld, Dry deposition parameterization in a chemistry general circulation model and its influence on the distribution of reactive trace gases, *J. Geophys. Res.*, *100*, 20,999–21,012, 1995.

Gathman, S. G., A preliminary description of NOVAM, the Navy Oceanic Vertical Aerosol Model, *NRL Rep. 9200*, Nav. Res. Lab., Washington, D. C., 1989.

Geernaert, G. L., and P. Astrup, Wind profile, drag coefficient, and radar cross section in the coastal zone for quasi-homogeneous conditions, in *The Wind Driven Air-Sea Interface*, edited by M. Banner, pp. 305–316, Univ. of New South Wales, Kensington, N. S. W., Australia, 1999.

Geernaert, L. L. S., G. L. Geernaert, K. Granby, and W. A. H. Asman, Fluxes of soluble gases in the marine atmospheric surface layer, *Tellus*, *Ser. B*, *50*, 111–127, 1998.

Gong, S. L., L. A. Barrie, and J.-P. Blanchet, Modeling sea-spray aerosols in the atmosphere, 1, Model development, *J. Geophys. Res.*, *102*, 3805–3818, 1997.

Hooper, W. P., and L. U. Martin, Scanning lidar measurements of surf-zone aerosol generation, *Opt. Eng.*, *38*, 250–255, 1999.

Hooper, W. P., J. E. James, and R. J. Lind, Lidar observations of turbulent vortex shedding by an isolated topographic feature, *Boundary Layer Meteorol.*, *80*(1–2), 95–198, 1996.

Katoshevski, D., A. Nenes, and J. H. Seinfeld. A study of processes that govern the maintenance of aerosols in the marine boundary layer, *J. Aerosol Sci.*, *30*(4), 503–532, 1999.

Low, R. D. H., A generalized equation for the solution effect in droplet growth, *J. Atmos. Sci.*, *26*(3), 608–611, 1969.

Marks, R., Preliminary investigation on the influence of rain on the production, concentration, and vertical distribution of sea-salt aerosol, *J. Geophys. Res.*, *95*, 22,299–22,304, 1990.

Monahan, E. C., and I. G. O'Muircheartaigh, Whitecaps and the passive remote sensing of the ocean surface, *Int. J. Remote Sens.*, *7*, 627–642, 1986.

Monahan, E. C., C. W. Fairall, K. L. Davidson, and P. J. Boyle, Observed inter-relations between 10 m winds, ocean whitecaps and marine aerosols, *Q. J. R. Meteorol. Soc.*, *109*, 379–392, 1983.

Monahan, E. C., D. E. Spiel, and K. L. Davidson, A model of marine aerosol generation via whitecaps and wave disruption, in *Oceanic Whitecaps and Their Role in Air-Sea Exchange Processes*, edited by E. C. Monahan and G. MacNiocaill, pp. 167–174, D. Reidel, Norwell, Mass., 1986.

North Sea Task Force, North Sea quality status report 1993, Olsen & Osen, Fredensborg, Denmark, 1993.

O'Dowd, C. D., M. H. Smith, I. E. Consterdine, and J. A. Lowe, Marine aerosol, sea salt, and the marine sulphur cycle: A short review, *Atmos. Environ.*, *31*, 73–80, 1997.

O'Dowd, C. D., et al., On the photochemical production of new particles in the coastal boundary layer, *Geophys. Res. Lett.*, *26*, 1707–1710, 1999.

Petelski, T., and M. Chomka, Marine aerosol fluxes in the coastal zone—BAEX experimental data, *Oceanologia*, *38*, 469–484, 1996.

Pruppacher, H. R., and J. D. Klett, *Microphysics of Cloud and Precipitation*, 954 pp., Kluwer Acad., Norwell, Mass., 1997.

Schulz, M., Fluxes across marine surfaces, in *Transport and Transformation of Pollutants in the Troposphere*, vol. 2, *Emissions, Deposition, Laboratory Work and Instrumentation*, edited by P. M. Borrell et al., pp. 45–49, Comput. Mech., Billerica, Mass., 1996.

Schwarz, S. E., Mass transport considerations pertinent to aqueous phase reactions of gases in liquid water clouds, in *Chemistry of Multiphase Atmospheric Systems*, *NATO ASI Ser.*, edited by W. Jaeschke, pp. 415–471, Springer-Verlag, New York, 1986.

Seinfeld, J. H., and S. Pandis, *Atmospheric Chemistry and Physics From Air Pollution to Climate Change*, 1326 pp., John Wiley, New York, 1998.

Slinn, S. A., and W. G. N. Slinn, Predictions for particle deposition on natural waters, *Atmos. Environ.*, *14*, 1013–1016, 1980.

Smith, M. H., M. K. Hill, P. M. Park, and I. E. Consterdine, Aerosol concentrations and estimated fluxes over the sea, in *Modeling the Fate and Influence of Marine Spray*, edited by P. G. Mestayer, E. C. Monahan, and P. A. Beetham, pp. 17–28, Mar. Sci. Inst., Univ. of Conn., Avery Point Groton, 1990.

Smith, M. H., P. M. Park, and I. E. Consterdine, Marine aerosol concentrations and estimated fluxes over the sea, *Q. J. R. Meteorol. Soc.*, *119*, 809–824, 1993.

Stramska, M., Vertical profiles of sea salt aerosol: A numerical model, *Acta Geophys. Pol.*, *35*, 87–100, 1987.

Stull, R., *An Introduction to Boundary Layer Meteorology*, 666 pp., Kluwer Acad., Norwell, Mass., 1988.

Vertegaal, C. T. M., Effecten van saltspray op flora en vegetatie—Mogelijke onderzoeksopzet (in Dutch), *Notitie Jan.*, 1998.

Vignati, E., Modelling interactions between aerosols and gaseous compounds in the polluted marine atmosphere, Ph.D. thesis, 133 pp., Dep. of Meteorol. and Wind Energy, Risø Natl. Lab., Roskilde, Denmark, 1999.

Vignati, E., G. de Leeuw, and R. Berkowicz, Aerosol transport in the coastal environment and effects on extinction, *Proc. SPIE Int. Soc. Opt. Eng.*, *3433*, 21–30, 1998.

R. Berkowicz, National Environmental Research Institute, Roskilde DK 4000, Denmark.

G. de Leeuw (corresponding author), Physics and Electronics Laboratory, TNO, P.O. Box 96864, 2509 JG The Hague, Netherlands. (deleeuw@fel.tno.nl)

E. Vignati, Environment Institute, Joint Research Centre, 21020 Ispra, Italy.

(Received October 30, 2000; revised March 15, 2001;
accepted April 13, 2001.)